Korean J. Chem. Eng., 35(2), 557-566 (2018)
DOI: 10.1007/s11814-017-0290-z

pISSN: 0256-1115
eISSN: 1975-7220

Microwave-assisted modification of activated carbon with cationic surfactants for enhancement of naphthalene adsorption

Zhonghai Sun, Zhansheng Wu†, Dandan Liu, and Xiufang He

School of Chemistry and Chemical Engineering/The Key Lab. for Green Processing of Chemical Engineering of Xinjiang Bingtuan, Shihezi University, Shihezi 832003, P. R. China
(*Received 4 July 2017 • accepted 12 October 2017*)

Abstract−Polycyclic aromatic hydrocarbons (PAHs) are toxic pollutants harmful to humans. To improve the adsorption capacity of PAHs on activated carbon (AC) from the aqueous system, AC was modified with cationic surfactants through microwave heating. Naphthalene is a typical PAH used as a model pollutant to test the adsorption properties of sample; the sample with the best adsorption performance was named SAC. The SAC was characterized by SEM, FTIR and BET in detail compared with AC. The specific surface area and the average pore size of SAC increased by nearly 100 m^2 g^{-1} and 0.14 nm more than the original AC, respectively. The adsorption experiment was carried out by batch technique with variables such as contact time, adsorbent amount, pH and temperature. Results showed that naphthalene was adsorbed rapidly during the first 20 min, and thereafter reached adsorption equilibrium in 40 min. The adsorption kinetics of naphthalene on SAC can be well described by the pseudo-second-order model and the Freundlich isotherm model better fitted the adsorption isotherms of naphthalene on SAC. Naphthalene adsorption process on SAC was spontaneous and temperature was found to negatively affect the adsorption capacity. Furthermore, film diffusion was confirmed the rate limiting step. The π-π stacking electron donor acceptor interaction, hydrophobic interaction and hydrogen bonding may play more key roles in naphthalene adsorption on SAC than AC. Thus, microwave-assisted surfactants modification was proven to be an effective method to enhance the adsorption of naphthalene onto SAC from aqueous solution.

Keywords: Activated Carbon, Naphthalene, Adsorption, Surfactant, Microwave

INTRODUCTION

Polycyclic aromatic hydrocarbons (PAHs) are a significant family of environmental pollutants composed of two or more fused aromatic rings. Often, they are formed from the incomplete combustion of hydrocarbons and other organic matters such as coal, petroleum, and biomass, all of which have been detected at elevated concentrations in municipal sewage and surface water [1-3]. Due to the high bioaccumulation and adverse health effects of PAHs, such as mutagenic, carcinogenic and teratogenic properties, they are classified as priority pollutants by the United States Environmental Protection Agency and the European Commission [2,4]. Owing to the poor biodegradability of PAHs, once they leak into the environment, they can exist for a long time [5,6]. Therefore, suitable methods for the removal of PAHs are needed.

Various techniques are currently being investigated to treat PAHs, such as biodegradation, sonication, membrane filtration, catalytic oxidation and photocatalytic degradation [7-9], but there are only few methods that are economical and efficient to remove PAHs from aqueous solutions [1,10]. Because adsorption systems are relatively easy to install and have low operation and maintenance costs [11], adsorption has demonstrated to be one of the most economical and attractive techniques for the removal of PAHs from aqueous solutions. Many studies have used different materials, such as activated carbon (AC), walnut shells, pine bark, and amorphous aluminum hydroxide, as adsorbent for the removal of PAHs [7, 12,13]. Among these materials, AC is the most commonly used adsorbent because of its unique and versatile pore structure, large specific surface area, abundant micro- and mesoporous structure, and high degree of surface reactivity [14-16]. The adsorption capacity of AC is influenced by its physical and chemical properties of AC [17,18]. However, the adsorption of PAHs by AC still has the problems of low removal rate and poor selectivity. Many researches have been focused on improving the adsorption capacity of AC to specific pollutants by modifying its microscopic structure and surface function groups [11-13]. Since PAHs are strongly non-polar and can be combined with hydrophobic adsorbents, therefore the increase of the hydrophobic interaction of AC and PAHs could be improving the adsorption ability of AC. Surfactants have an amphipathic structure with a hydrophobic tail and a hydrophilic head, and have been applied to modify the characteristics of a solid surface [19]. Recently, some studies demonstrated that AC was modified through surfactants to adsorb pollutants [11,19-21]. Granular activated carbon (GAC) modified with a cationic surfactant has been reported and found that modified GAC could enhance GAC's adsorption for bromate [11]. Cationic surfactant cetyltrimethyl ammonium bromide was applied to the modified carbon powder as an efficient sorbent for cadmium removal from aqueous solu-

†To whom correspondence should be addressed.
E-mail: wuzhans@126.com

tion [20]. In addition, the adsorption capacity of cationic surfactant-modified AC for Cr(VI) was enhanced compared to AC [21]. However, cationic surfactant modified AC used for removing PAHs from solution has never been reported. In addition, AC is known to be a good microwave absorber [12], and microwave-assisted modification of AC is very interesting and valuable. Thus, the investigation of cationic surfactant-modified AC by microwave assisted in improving the adsorption capacity of PAHs is an innovative and significant attempt.

We used naphthalene as one of the typical PAHs as an object of adsorbate. Our aim was to investigate the feasibility of modification of AC using cationic surfactants for enhancing its adsorption properties of naphthalene from aqueous solutions. The structural characteristics of samples were analyzed using scanning electron microscopy (SEM), nitrogen adsorption-desorption and Fourier transform infrared spectroscopy (FTIR). The adsorption capacities and adsorption behavior of naphthalene on SAC were examined through adsorption kinetics and isotherms compared with AC. Meanwhile, the mechanism and thermodynamics were considered for the adsorption studies. This study not only provides an efficient method for the removal of naphthalene, but also provides useful information for the treatment of other complicated PAHs.

EXPERIMENTAL

1. Materials and Reagents

AC was obtained by microwave radiation from coal according to our previous study [5]. Raw coal was supplied by Tebian Electric Apparatus, Xinjiang Uygur Autonomous Region, China. Then, the prepared AC was washed with 10% hydrochloric acid and distilled water until the filtrate reached neutrality. The resulting black power was dried in an oven overnight at 383.15 K for further modification. Cationic surfactants Dodecyltrimethylammonium chloride (DTAC), Cetyltrimethylammonium chloride (CTAC) and Stearyl trimethyl ammoium chloride (STAC) were purchased from Aladdin Industrial Corporation. All other chemicals and reagents used were of analytical grade.

2. Modification of AC

1 g of AC was added to a 250 mL round bottom flask with 50 mL of different kinds of 10 mM surfactant solutions (DTAC, CTAC and STAC) and then mixed homogeneously. The mixtures were heated at 343.15 K for 20 min in microwave reactor (MCR-3, China), which is an instrument using continuous microwave output and adaptive proportional-integral-derivative (PID) regulation technology. After modification, the mixture was filtered and washed with distilled water, dried in an oven at 383.15 K for 4 h, and then named DTAC-AC, CTAC-AC and STAC-AC, used for further study, respectively. After the better surfactant was selected, the factor of different concentrations of surfactant solution (1, 10, 20 and 50 mM) was explored according to the above research method. The adsorbent was characterized by various analytical techniques.

3. Characterization

FTIR analysis of the adsorbent before and after modification of AC by surfactants was in the range of 4,000-400 cm^{-1} with 4 cm^{-1} resolution using PHI5700 ESCA infrared spectrometer and by applying a KBr pellet technique.

The micrographs and pore structure of the adsorbents were obtained using SEM (JEOL, JSM-6490LV, Japan) at an acceleration voltage of 15 kV. The samples were sprayed with gold prior to the test.

The specific surface area and pore distributions of samples were measured at 77 K on Micromeritics model ASAP 2020 sorptometer that uses nitrogen adsorption-desorption isotherms. Pore-size distributions were obtained by the BJH method, and the specific surface area of the samples was calculated by BET method.

The point of zero charge (pH_{pzc}) of AC and SAC was measured according to the procedure described by Cabal and Budinova [3]. The pH_{PZC} is the point where $pH_{initial}$-pH_{final} versus pH initial was zero.

4. Batch Adsorption Studies

4-1. Adsorption Studies for Optimization of Modification Conditions

In this experiment, 0.0400 g of modified samples (DTAC-AC, CTAC-AC and STAC-AC) were contacted with 100 mL of naphthalene solution with concentration 30 mg L^{-1} and the mixture was shaken with 170 rpm agitation speed at 298.15 K for 60 min, assuming that adsorption equilibrium had been reached by that time (kinetic tests indicated that sorption equilibrium was achieved in less than 60 min). The treated solution was then separated by centrifugation at 10,000 rpm for 10 min, and the concentrations of the supernatant were measured using a UV-752N spectrophotometer at 219 nm wavelength (λ_{max}). Each experiment was carried out in triplicate and each analysis of naphthalene concentration was also performed in triplicate. The removal efficiency was calculated using the average of the three data. According to this result, the best surfactant was selected. For the choice of modifier concentration, similar procedures were conducted at different concentrations of modified samples (0, 1, 10, 20 and 50 mM), with the other conditions remaining constant. The removal rate (%) was calculated based on the following equation:

$$\text{Removal (\%)}=(C_o-C_e)/C_o \quad (1)$$

where C_o and C_e denote the initial and equilibrium concentrations (mg L^{-1}), respectively.

The adsorption capacity of naphthalene at equilibrium q_e (mg g^{-1}) can be calculated by the following equation:

$$q_e=(C_o-C_e)\times V/m \quad (2)$$

where q_e is the amount of naphthalene adsorbed by AC or modified AC (mg g^{-1}), V is the volume of the aqueous solution (L), and m is the mass of the adsorbent (g).

4-2. Kinetic Studies and Adsorption Isotherms

The influence on the adsorbent amount for the adsorption of naphthalene was studied, at a fixed the 100 mL initial concentration of 30 mg L^{-1} naphthalene solution, then the adsorbent amount was varied from 0.0100 to 0.0400 g and shaken for 60 min at 298.15 K with 170 rpm agitation speed. Adsorption kinetic experiments were conducted in conical flasks at 298.15 K. Briefly, 0.0150 g of adsorbent was contacted with 100 ml of aqueous solutions with the concentrations of 30 mg L^{-1} naphthalene and the samples were taken out at different contacting time intervals (2-160 min).

For the adsorption isotherms and thermodynamic studies, similar procedures were carried out at different temperatures (288.15, 298.15 and 308.15 K) and naphthalene concentrations (5-50 mg L^{-1}), respectively, with the other factors remaining constant. To verify the effect of solution pH, a 2-12 pH range was selected by using a constant initial naphthalene concentration (30 mg L^{-1}) and adsorbent dosage (0.0150 g) at 298.15 K for 60 min with the agitated speed of 170 rpm. After sorption, the solution and adsorbents were treated according to the method in Section 2.4.1.

5. Data Analysis

5-1. Adsorption Kinetics

To investigate the interaction between solutes on the surface of the adsorbents during adsorption process, two kinetic models, pseudo first-order and pseudo-second-order models were employed to analyze the experimental data and predict the adsorption kinetic behaviors in this work. The nonlinear equation form for the pseudo first-order model [22] is described as follows:

$$q_t = q_e(1-\exp^{-k_1 t}) \quad (3)$$

where q_t and q_e are the adsorption amounts of naphthalene on sorbent (mg g^{-1}) at time t (min) and equilibrium, respectively, and k_1 (min^{-1}) is the pseudo-first-order adsorption rate constant.

The nonlinear equation form for the pseudo-second-order model [23] is expressed as: (4)

$$q_t = q_e^2 k_2 t/(1+q_e k_2 t) \quad (4)$$

where k_2 (g $mg^{-1}min^{-1}$) is the rate constant of the pseudo second-order model.

To find a suitable kinetic model to describe the adsorption behavior, the determination coefficient (R^2) and the residual root-mean squared error (RMSE) were used to evaluate the pseudo-first-order and pseudo second-order models. R^2 and RMSE can be expressed by Eqs. (5) and (6) [16,24]:

$$R^2 = 1-\Sigma_{n=1}^{n}(q_{t,\,exp,\,n}-q_{t,\,cal,\,n})^2/\Sigma_{n=1}^{n}(q_{t,\,exp,\,n}-\overline{q_{t,\,exp,\,n}})^2 \quad (5)$$

$$RMSE = \sqrt{(1/(n-1))\Sigma_{n=1}^{n}(q_{t,\,exp,\,n}-q_{t,\,cal,\,n})^2} \quad (6)$$

where $q_{t,exp}$ and $q_{t,cal}$ (mg g^{-1}) are the experimental adsorption capacities and theoretical calculated adsorption capacities from the model at time t, respectively, and n represents the number of experiments. A better fitted model can be predicted with high R^2 and low RSME.

5-2. Adsorption Isotherm Models

To study the distribution of adsorbate on the surface of the adsorbent, the Langmuir [25] and Freundlich [26] isotherm models were employed to determine the adsorption isotherm parameters of naphthalene on SAC. The nonlinear form of equation for the Langmuir model is described in Eq. (7) and the Freundlich model can be expressed in nonlinear form as Eq. (9):

$$q_e = q_{max}K_L C_e/(1+K_L C_e) \quad (7)$$

$$R_L = 1/(1+K_L C_e) \quad (8)$$

$$q_e = K_F C_e^{1/n} \quad (9)$$

where K_L (L mg^{-1}) is the adsorption coefficient of the Langmuir model involved in the energy of adsorption and q_{max} (mg g^{-1}) is the maximum adsorption capacity at saturation; R_L is the Langmuir separation factor; K_F ($mg^{1-1/n}$ $L^{1/n}$ g^{-1}) is the adsorption constant of the Freundlich model and n exponential coefficient indicates the favorable adsorption ability.

The applicability of the models was determined by R^2 and RMSE function values, the R^2 and RMSE are described using Eqs. (10) and (11) [16,24]:

$$R^2 = 1-\Sigma_{n=1}^{n}(q_{e,\,exp,\,n}-q_{e,\,cal,\,n})^2/\Sigma_{n=1}^{n}(q_{e,\,exp,\,n}-\overline{q_{e,\,exp,\,n}})^2 \quad (10)$$

$$RMSE = \sqrt{(1/(n-1))\Sigma_{n=1}^{n}(q_{e,\,exp,\,n}-q_{e,\,cal,\,n})^2} \quad (11)$$

where $q_{e,exp}$ and $q_{e,cal}$ (mg g^{-1}) are the experiment adsorption capacity and the predicted adsorption capacity at equilibrium time, respectively.

5-3. Adsorption Thermodynamics

To investigate the effect of temperature on the adsorption process of naphthalene onto sorbent, thermodynamic parameters containing Gibbs free energy change (ΔG), enthalpy change (ΔH) and entropy change (ΔS) were determined employing the following equations [27]:

$$\Delta G = -RT\ln K_o \quad (12)$$

$$K_o = H_e/C_e \quad (13)$$

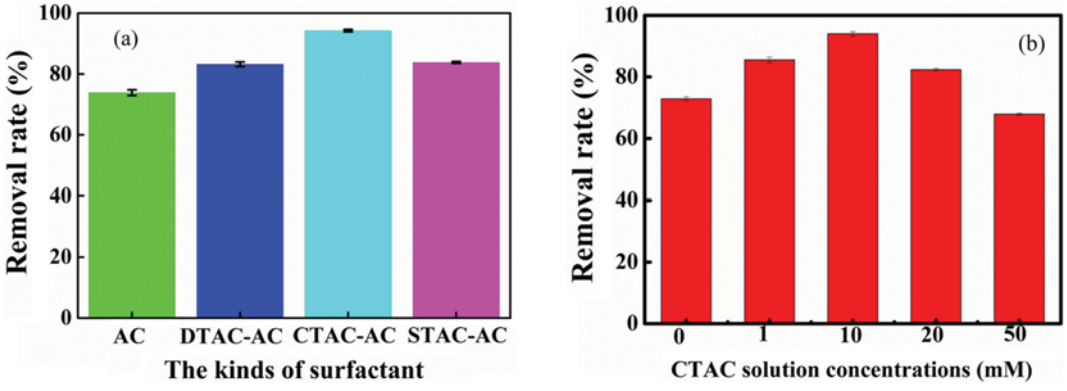

Fig. 1. Effects of the modification conditions on modified AC for naphthalene adsorption: (a) The kinds of surfactant; (b) CTAC solution concentrations (amount of adsorbent, 0.0400 g; contact time, 60 min; agitation speed, 170 rpm; the concentration of naphthalene, 30 mg L^{-1}).

$$\ln K_o = -\Delta G/RT = \Delta S/R - \Delta H/RT \quad (14)$$

where H_e is the equilibrium concentration of naphthalene on AC or SAC (mg L^{-1}), C_e is the concentration of naphthalene at equilibrium in the solution (mg L^{-1}), K_o is the equilibrium constant, R is the universal gas constant (8.314 J $mol^{-1}K^{-1}$), and T is the solution temperature (K).

RESULTS AND DISCUSSION

1. Effect of the Surfactant Types on the Modification of AC

The percentage removal of naphthalene at the initial concentration 30 mg L^{-1} in 298.15 K was 74.80%, 83.35%, 94.35% and 83.77% for AC, SATC-AC, CTAC-AC and DTAC-AC, respectively (Fig. 1(a)). All other parameters were the same as described in the experimental. CTAC-AC was found to be the best sample among the tested. Compared with CTAC, STAC may be ascribed to the increase in the alkyl chain length and the complicated arrangement of quaternary ammonium cations in AC because of the steric effect, which results in the reduced adsorption removal rate of naphthalene, while DTAC has a short alkyl chain, which makes aggregating in the solution difficult because of the strong hydrophilicity [28]. Therefore, CTAC was selected as the best modifier for further experiments.

2. Effect of the Surfactant Concentration on the Modification of AC

The different concentration surfactant CTAC was investigated to modify AC (Fig. 1(b)). The adsorption capacity of the modified AC was increased with the increase of CTAC concentration, and the removal rate of naphthalene was maximized at the concentration of 10 mM CTAC. However, the removal rate of naphthalene adsorbed decreased from 94.35% to 67.91% when the concentration was increased from 10 to 50 mM. This phenomenon was caused by the excessive amounts of surfactant that clogged the aperture [11], and thus resulted in decreased adsorption efficiency. To obtain a high removal rate of modified AC for naphthalene, 10 mM CTAC solution was selected as the appropriate concentration for modification; this modified AC sample was named as SAC.

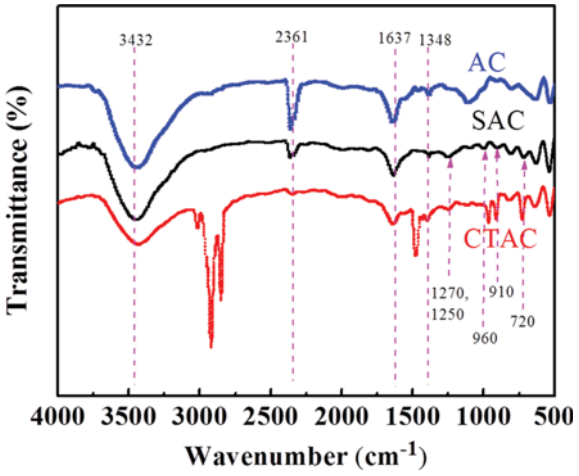

Fig. 2. The FT-IR spectrum of samples.

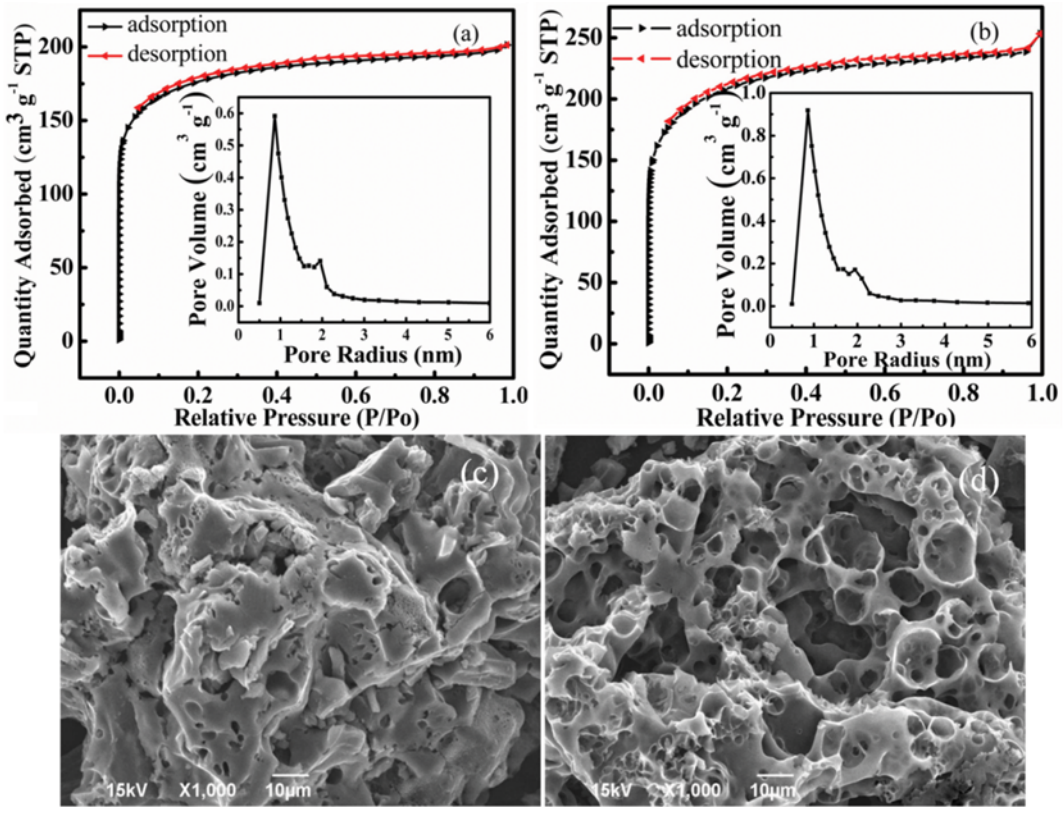

Fig. 3. The characterization of BET and SEM for samples: (a) and (c) for AC, (b) and (d) for SAC.

3. Characterization

3-1. FTIR Spectra Analysis

The samples were characterized with FTIR to reveal the change in active functional groups on the SAC surface (Fig. 2). The wide and strong band of SAC at approximately 3,432 cm^{-1} was attributed to the stretching vibration of hydroxyl groups, which indicated the existence of a phenolic group [16,17]. The difference in intensity of the 2,361 cm^{-1} band between AC and SAC indicated that the modification process caused C-O groups to decrease [5,12]. The band at 1,637 cm^{-1} corresponded to the strong asymmetric vibration of C-O-O bending, and the band at 1,384 cm^{-1} was caused by the weak symmetric stretching vibration of C-O-O [14,16]. Compared with the FTIR spectra of AC, additional peaks appeared at 1,270, 1,250, 960, 910 and 720 cm^{-1} in SAC, which correspond to C-O stretching vibration, in-plane bending vibration of C-H, unsaturated C-H in-plane bending vibration and C-Cl stretching vibration of alkyl halide after the interactions in the modification process [17]. Thus, it can be inferred that CTAC modified AC successfully.

3-2. Surface Area Analysis

The N_2 adsorption-desorption isotherm curves of AC and SAC at 77 K are illustrated in Fig. 3(a) and (b). The overall shape of the isotherm curves of the samples exhibited a typical type I, showing a slow increase in high relative pressures (P/P_0), but a sharp rise in low relative pressures depicts proved AC and SAC may be micropore materials. Meanwhile, a small hysteresis loop was likewise observed at high relative pressure, indicating the inherent mesoporosity of the material [3,14]. From Table 1, the specific surface area of SAC was significantly improved more than AC, which increased by nearly 100 $m^2\ g^{-1}$; this may lead to its enhancement of adsorption capacity for naphthalene. Nadeem [20] similarly reported that carbon powder modified with cationic surfactant increased the BET surface area from 725.0 to 814.2 $m^2\ g^{-1}$ and enhanced the adsorption for cadmium. Meanwhile, the micropore surface area of SAC was nearly the same as that of the original AC, but the external surface area clearly increased after surfactant modification, which may be due to the presence of porosity in surfactants that have been loaded on the surface of AC [20]. Moreover, the average pore sizes of AC and SAC were found to be 0.79 and 0.93 nm, respectively. This finding suggested that the average pore size increased after the modification process and it would be conducive to naphthalene adsorption [5,12]. This is because the increased pore size of the modified sample is more suitable for entrance of naphthalene (the molecular dimension: 0.91×0.73×0.38 nm). The mesoporous volume and total pore volume increased after modification, which might be beneficial for adsorption. Ge [12] found that microwave radiation modified coal-based activated carbon (CAC) to form mesopores and became more effective for the adsorption of PAHs from the aqueous solutions. Therefore, we assumed that the developed pore properties and formed mesopores may enhance the adsorption for naphthalene.

3-3. SEM Analysis

The morphologies and porous structure of the AC and SAC were determined from the SEM (Fig. 3(c) and (d)). An uneven and rough surface morphology was observed on the unmodified AC, which had poor pore structure. The SEM image indicates that the surfactant modified sample enriched the pore structure by microwave assisted method, which contributed to the adsorption capacity of SAC for naphthalene. Previous study had been observed that SDS modified ordered nanoporous carbon can be increased the adsorption of methylene blue [20]. In addition, the homogeneous circular appearance with different sizes of pores distributed on the surface is mainly responsible for naphthalene adsorption onto the SAC surface [12,13].

4. Adsorption

4-1. Effect of Adsorbent Amount for Naphthalene Adsorption

To find the optimum amount of adsorbent for the adsorption

Table 1. Surface characteristic of AC and SAC

Sample	S_{BET} ($m^2\ g^{-1}$)	A_m ($m^2\ g^{-1}$)	A_e ($m^2\ g^{-1}$)	V_{mic} ($cm^3\ g^{-1}$)	V_{mes} ($cm^3\ g^{-1}$)	V_t ($cm^3\ g^{-1}$)	Average pore radius (nm)	pH_{PZC}
AC	660.60	436.43	224.17	0.17	0.14	0.31	0.79	5.92
SAC	757.19	437.74	329.86	0.18	0.21	0.39	0.93	6.35

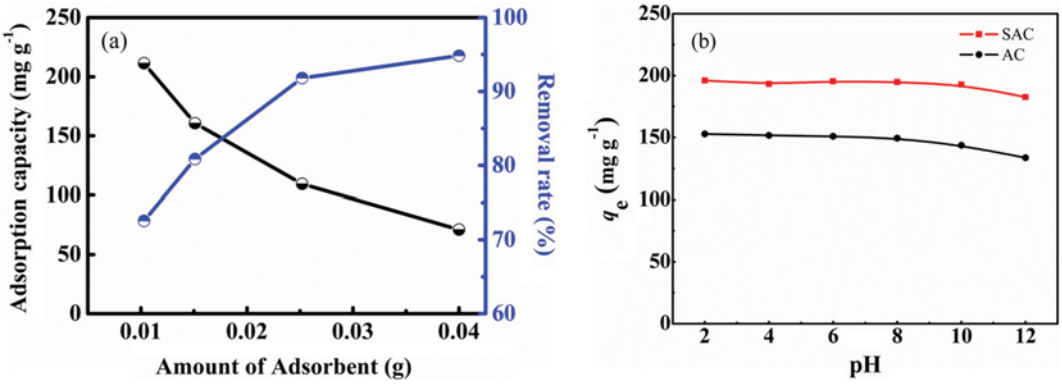

Fig. 4. Effect of adsorbent amount (a) and the pH (b) for naphthalene adsorption (contact time, 60 min; agitation speed, 170 rpm; the concentration of naphthalene, 30 mg L^{-1}).

process, the adsorbent amount was varied from 0.0100 to 0.0400 g for 100 mL of 30 mg L^{-1} naphthalene solution. Fig. 4(a) illustrates that the removal rate increased with increasing of adsorbent amount; it might be due to that the higher amount of the adsorbent provides more effectively surface area and more active sites [16]. However, the capacity of the adsorbent decreased with a higher amount of adsorbent; it may be that the excessive sites had not been fully utilized [12]. Therefore, considering the relationship between the adsorption capacity and the removal rate, a small amount of adsorbent has high adsorption efficiency, and 0.0150 g was selected as the optimum amount of adsorption for the next step of the study.

4-2. Effect of pH

Fig. 4(b) illustrates the effect of solution pH on naphthalene adsorption of AC and SAC at 298.15 K. The results show that the adsorption capacity of SAC and AC on naphthalene decreases with the increase of pH, and acidic conditions contribute to adsorption. When the pH changed from 2 to 12, the adsorption capacity of SAC to naphthalene decreased from 192.06 to 182.65 mg g^{-1}. The pH_{pzc} of SAC (6.35) plays an important role in determining the performance. Thus, at low pH, the surface charge of adsorbent was positively charged, which enhanced the adsorption through electrostatic forces of attraction between the positively charged adsorbent surface and naphthalene [16]. In contrast, at higher pH, adsorption of OH^- ions and naphthalene at the same adsorption site may also result in lower adsorption. Similar result was obtained by Gupta [2] for removal of naphthalene using AC based on banana peel.

4-3. Adsorption Kinetics

Fig. 5 presents the adsorption kinetics for naphthalene removal on AC and SAC at 298.15 K by plotting adsorption capacity versus time t. The SAC had a faster adsorption rate in the first 20 minutes compared to AC, while there was almost no significant change after 20 min, and adsorption equilibrium was finally reached at 40 min. The initial rapid adsorption may be attributed to the abundant available active sites at the beginning of contact; with the proceeding of the adsorption, because of the accumulation of naphthalene adsorbed on the surface sites, the driving forces caused by concentration gradient were reduced [16]. According to the high R^2 values and the low RMSE in Table 2, the pseudo-second-order model fitted the adsorption kinetic of naphthalene on AC and SAC much better than the pseudo-first-order model. Meanwhile, the experimental equilibrium adsorption capacity $q_{e,exp}$ was more consistent with the calculated $q_{e,cal}$ from the pseudo-second-order model. This result indicates that the naphthalene adsorption process may be involving chemical adsorption. Previous results reported that the adsorption of PAHs on the CAC and fatty acid modified walnut shell [12,13] also supported the pseudo-second-order model.

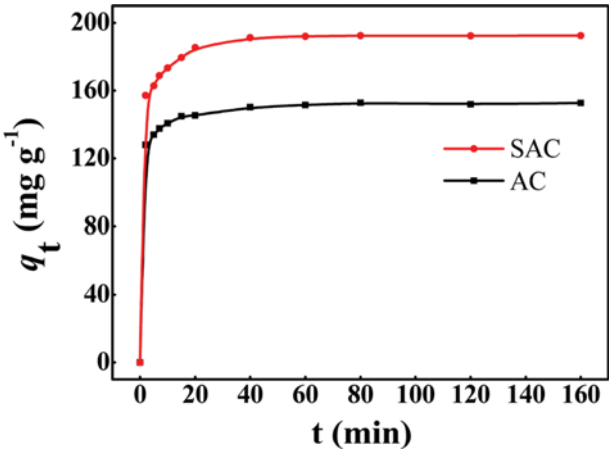

Fig. 5. The effect of contact time on the adsorption kinetic modeling for the adsorption of naphthalene by AC and SAC (V=100 mL, m=0.0150 g, shaking speed of 170 rpm).

To assess further the adsorption mechanisms and to determine the resistance of mass transfer, the Webber and Morris intraparticle diffusion model [29] was established to analyze the adsorption process, and the model is expressed as:

$$q_t = K_{id} t^{0.5} + C \quad (15)$$

where C is the constant of boundary layer involving thickness and K_{id} is the rate constant of intraparticle diffusion (mg g^{-1} $min^{-0.5}$). The linearity of data in q_t versus $t^{0.5}$ plot illustrated the intraparticle diffusion process mechanism.

The Boyd model [30] was applied to distinguish the adsorption process as intraparticle diffusion or film diffusion and to identify the rate-limiting step. The Boyd equation can be expressed as:

$$-\ln(1-q_t/q_e) = K_{fd} t \quad (16)$$

where K_{fd} is liquid film diffusion constant.

According to Fig. 6(a) and the R^2 of intraparticle diffusion shown in Table 3, the curves are mulitilinear at the entire range. This phenomenon indicates that intraparticle diffusion is not the only slowest step in the adsorption process, but other processes may be involved in the adsorption reaction. From Fig. 6(a), two separate regions can be clearly observed. The first part can be ascribed to the instant boundary layer diffusion where naphthalene adsorption rate is high due to large amounts of active sites and low competition between the naphthalene. The second part may be related to the intraparticle diffusion, through the first part. The naphthalene has diffused to the interior surface of the particles where the naphthalene adsorption rate has gradually slowed and then reached the equilibrium because of the decrease of concentration driving

Table 2. Kinetic parameters for naphthalene adsorption on AC and SAC

Sample	$q_{e,exp}$ (mg g^{-1})	Pseudo-first-order model				Pseudo-second-order model			
		k_1 (min^{-1})	$q_{e,cal}$ (mg g^{-1})	R^2	RMSE	k_2	$q_{e,cal}$ (mg g^{-1})	R^2	RMSE
AC	152.831	0.992	146.478	0.978	6.020	0.015	150.680	0.994	3.026
SAC	192.502	0.904	183.659	0.963	9.887	0.009	190.332	0.989	5.341

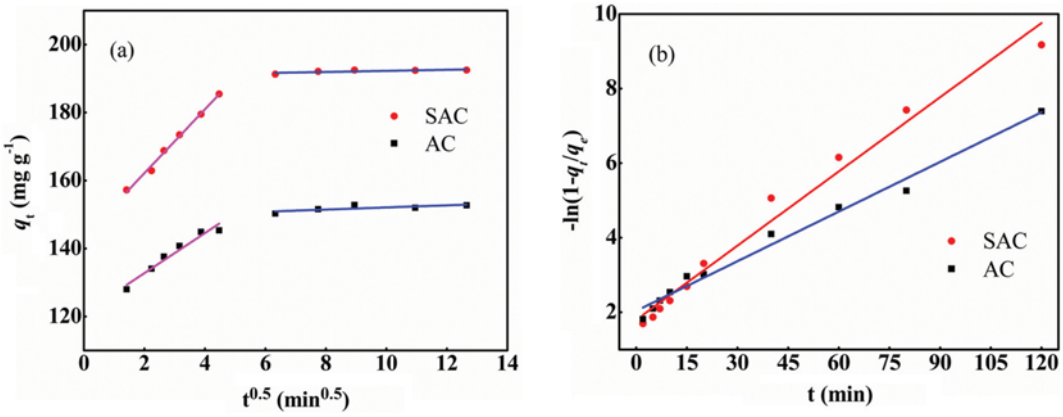

Fig. 6. Weber and Morris intraparticle diffusion (a) and Boyd film diffusion (b) plot for the adsorption naphthalene by AC and SAC at 298.15 K.

Table 3. Intraparticle diffusion and film diffusion parameters at 298.15 K

Sample	Intraparticle diffusion model				Film diffusion model	
	Step 1		Step 2		K_{fd}	R^2
	K_{id}	R^2	K_{id}	R^2		
AC	5.894	0.948	0.312	0.638	0.044	0.983
SAC	9.392	0.993	0.159	0.693	0.066	0.979

forces. Meanwhile, the Boyd model data of $-\ln(1-q_t/q_e)$ versus t are exhibited in Fig. 6(b). Obviously, the Boyd plots are linear but do not pass the origin, suggesting that film diffusion is the rate-limiting step and liquid film diffusion resistance plays an important role in the adsorption process. In addition, an analysis of the data in Table 3 shows that the R^2 of film diffusion was significantly higher than the values of intraparticle diffusion model. This result from the other side illustrated that film diffusion is the rate-limiting step of adsorption naphthalene in AC and SAC under the studied conditions.

4-4. Effect of Temperature

To investigate the effect of interaction temperature for the naphthalene adsorption on the adsorbents, experiments were carried out at 288.15, 298.15 and 308.15 K. Fig. 7(a) shows that the adsorption amount of AC and SAC decreased with the increase in temperature. This trend indicates that the adsorption behavior of naphthalene of AC and SAC is exothermic. Previous researches found similar results for the adsorption PAHs on AC [5,12].

To further assess the effect of temperature on adsorption, detailed data analysis of adsorption thermodynamics was utilized to discuss the adsorption behavior. Fig. 7(b) demonstrates the relationship between ln K_o and $-1/T$, which are the thermodynamic par-

Table 4. The thermodynamic parameters for the adsorption of naphthalene onto AC and SAC

Adsorbent	Temperature (K)	ΔH (kJ mol^{-1})	ΔS (J mol^{-1}K^{-1})	ΔG (kJ mol^{-1})
AC	288.15	−13.85	−37.75	−2.97
	298.15			−2.59
	308.15			−2.22
SAC	288.15	−23.90	−57.87	−7.72
	298.15			−6.65
	308.15			−6.07

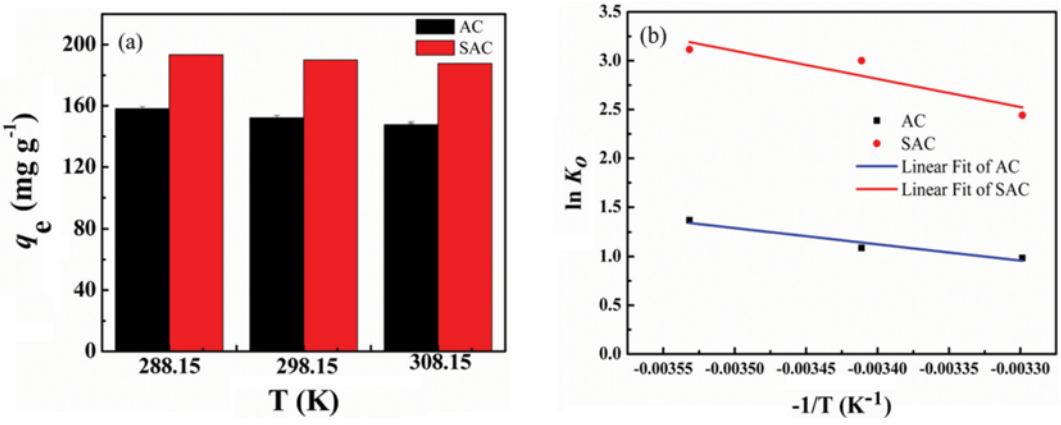

Fig. 7. The reaction temperature (a) and and the thermodynamic plots of ln K_o versus $-1/T$ (b) for the adsorption of naphthalene by AC and SAC.

ameters that can be calculated by the slope and intercept following Gibbs and van't Hoff Eqs. (12), (13), (14) and summarized in Table 4. The value of ΔH is negative, suggesting the exothermicity of the adsorption process of the naphthalene onto adsorbents, which is supported by the decrease of adsorption capacity with the increase of temperature (as shown in Fig. 7(a)). The negative value of ΔS reflects that the decreased randomness of the adsorbents affinity of naphthalene at solid and liquid interface during the adsorption process, perhaps because of naphthalene attached to the functional groups of the sample surface and which can be explained through the experiment. In addition, the ΔG are negative at all the test temperatures (288.15-303.15 K), confirming that the naphthalene adsorption is a spontaneous process. Furthermore, the ΔG decreases with increasing temperature, suggesting that adsorption is more efficient at lower temperature. Moreover, all thermodynamic parameters of SAC are less than these of AC, which indicates that the adsorption of naphthalene is more likely to occur in SAC under the same conditions. The values of ΔG obtained were between −20 and 0 kJ mol^{-1}, which implies that adsorption procedures may be involved in physisorption [31]. Therefore, the adsorption of naphthalene on AC and SAC is exothermic and spontaneous, and high temperature is unfavorable in this process which possibly is driven by physisorption.

4-5. Equilibrium Adsorption Isotherm Studies

Fig. 8 presents the adsorption isotherms of naphthalene on AC and SAC as a relationship between q_e and C_e at 298.15 K. As shown in Fig. 8, the adsorption capacity increases with increasing initial concentration due to the significant driving forces caused by concentration gradient. The parameters of Langmuir and Freundlich isotherm models are summarized in Table 5. A good agreement between the parameters was evaluated with the high value of R^2 and low RMSE. The adsorption process of naphthalene on SAC is better fitted by the Freundlich model, which indicated that the removal of naphthalene on the heterogeneous surface of SAC may be related to multilayer adsorption that also sustains physical adsorption [17]. This indicated that CTAC surfactant (as active site) may be dispersed on the surface of AC. The 1/n values obtained from the Freundlich model were <1, which indicates a favorable adsorption process and SAC having a smaller 1/n value relative to AC implies a better ability for adsorption [16]. This result shows the better dispersed capability of surfactant via microwave modification method. Moreover, the R_L of the Langmuir parameter also represents the shape of the adsorption isotherm and the irreversible procedure for R_L=0; the adsorption is favorable when the value of R_L is between 0 and 1 [15]. From Table 4, the calculated R_L values were in the range of 0.400-0.928 and 0.321-0.915, respectively. It may be inferred that naphthalene adsorption on AC and SAC is favorable because the values are greater than 0 and less than 1 [15].

4-6. Adsorption Mechanisms

We also investigated the interaction behavior of naphthalene and adsorbent. As a structure with hydrophilic head toward the inside and hydrophobic tail toward the outside was formed on the surface of AC, which may be because of the electrostatic effect between the cationic group of CTAC and the surface of AC, it was conducive to the capture of naphthalene by the hydrophobic interaction. In the case of naphthalene adsorption, the electron donor acceptor interaction may occur by the π-π stacking interaction [13,32]. The aromatic ring of SAC provided adsorption sites with high adsorption affinity towards aromatic compounds, including naphthalene through the π-π stacking electron donor acceptor interaction and face-to-face π-π stacking interaction do not occur, a T-shape interaction may occur [33]. Similar results have been observed for the adsorption of PAHs using pine bark, plant resi-

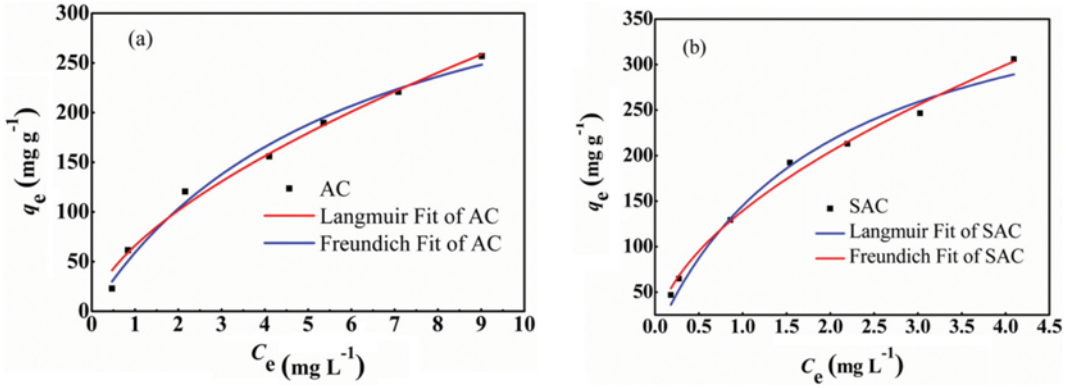

Fig. 8. Langmuir and Freundlich isotherms for naphthalene onto AC and SAC at 298.15 K (shaking speed, 170 rpm; contact time, 40 min; adsorbent, 0.0150 g).

Table 5. Langmuir and Freundlich parameters for adsorption of naphthalene on AC and SAC

Sample	Langmuir					Freundlich			
	q_{max}	K_L	R_L	R^2	RMSE	K_F	1/n	R^2	RMSE
AC	403.838	0.166	0.400-0.928	0.985	9.543	66.049	0.621	0.994	5.365
SAC	436.210	0.516	0.321-0.915	0.980	11.924	139.362	0.552	0.991	9.015

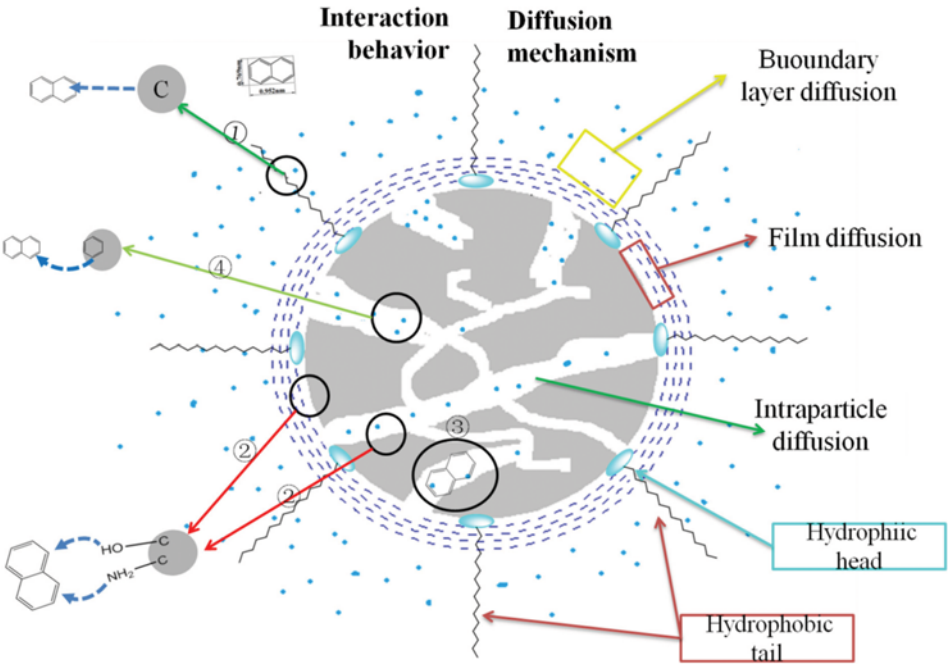

Fig. 9. The purpose mechanism of naphthalene adsorption on SAC, including the action behavior: ① Hydrophobic attraction with hydrophobic tails of CTAC; ② H-bond with hydroxyl groups and amino groups on SAC; ③ hydrophobic attraction on oxygen and nitrogen functional groups; ④ π-π stacking electron donor acceptor interactions with the aromatic ring of SAC.

due materials and walnut shells and so on [1,7,13]. Owing to the presence of oxygen and nitrogen functional groups of AC and SAC, a hydrophobic structure was formed and the average pore diameters of AC and SAC were 0.79 and 0.93 nm, respectively. So, as compared with AC, the SAC has more suitable pore size beneficial to naphthalene adsorption by hydrophobic interaction [32]. Meanwhile, hydrogen bonding may exist between amino groups and hydroxyl groups and naphthalene [10]. The proposed mechanisms of naphthalene on AC and SAC according to the above discussion are shown in Fig. 9.

CONCLUSIONS

The adsorption properties of AC and SAC were investigated using naphthalene. Pore structural and functional tests (SEM, BET and FT-IR) indicated that SAC has a developed pore structure, and the specific surface area clearly improved. Furthermore, the surfactant may be loading on the surface compared with AC through microwave-assisted method. The kinetics with AC and SAC illustrated a similar trend: the adsorption rate was fast in the first 20 min, and then adsorption reached equilibrium after 40 min of contact time, as well the SAC (192.50 mg g^{-1}) showed higher adsorption ability than AC (152.83 mg g^{-1}). The kinetic model of the pseudo second-order best described the kinetic data for AC and SAC, and the adsorption thermodynamic data indicated that the adsorption is exothermic and low temperature is better for this process. Conclusively, the microwave-assisted surfactant modifying proposal could improve the microstructure and surface properties of AC for enhancing its adsorption of naphthalene, which has the potential for industrial application.

ACKNOWLEDGEMENTS

This work was supported financially by funding from the International Scientific and Technological Cooperation Project of Xinjiang Bingtuan (2013BC002) and the International Science and Technology Cooperation Program of Shihezi University (GJHZ201601).

REFERENCES

1. B. Chen, M. Yuan and H. Liu, *J. Hazard. Mater.*, **188**, 436 (2011).
2. H. Gupta and B. Gupta, *Desalin. Water. Treat.*, **30**, 1 (2015).
3. B. Cabal, T. Budinova, C. O. Ania, B. Tsyntsarski, J. B. Parra and B. Petrova, *J. Hazard. Mater.*, **161**, 1150 (2009).
4. K. Amstaetter, E. Eek and G. Cornelissen, *Chemosphere*, **87**, 573 (2012).
5. X. Xiao, D. Liu, Y. Yan, Z. Wu, Z. Wu and G. Cravotto, *J. Taiwan Inst. Chem. E.*, **53**, 160 (2015).
6. C. Long, J. Lu, A. Li, D. Hu, F. Liu and Q. Zhang, *J. Hazard. Mater.*, **150**, 656 (2008).
7. Y. Li, B. Chen and L. Zhu, *Bioresour. Technol.*, **101**, 7307 (2010).
8. D. T. Sponza and R. Oztekin, *Bioresour. Technol.*, **101**, 8639 (2010).
9. R. J. Krupadam, *Environ. Chem. Lett.*, **9**, 389 (2011).
10. W. Chen, L. Duan, L. Wang and A. D. Zhu, *Environ. Sci. Technol.*, **42**, 6862 (2008).
11. W.-f. Chen, Z.-Y. Zhang, Q. Li and H.-Y. Wang, *Chem. Eng. J.*, **203**, 319 (2012).
12. X. Ge, F. Tian, Z. Wu, Y. Yan, G. Cravotto and Z. Wu, *Chem. Eng. Process.*, **91**, 67 (2015).
13. M. Zhu, J. Yao, L. Dong and J. Sun, *Chemosphere*, **144**, 1639 (2016).
14. R. H. Hesas, A. Arami-Niya, W. M. A. W. Daud and J. N. Sahu, *J.*

Anal. Appl. Pyrol., **104**, 176 (2013).
15. K. C. Bedin, A. C. Martins, A. L. Cazetta, O. Pezoti and V. C. Almeida, *Chem. Eng. J.*, **286**, 476 (2016).
16. A. Benhouria, M. A. Islam, H. Zaghouane-Boudiaf, M. Boutahala and B. H. Hameed, *Chem. Eng. J.*, **270**, 621 (2015).
17. V. O. Njoku, M. A. Islam, M. Asif and B. H. Hameed, *J. Anal. Appl. Pyrol.*, **110**, 172 (2014).
18. R. H. Hesas, A. Arami-Niya, W. M. A. W. Daud and J. N. Sahu, *J. Ind. Eng. Chem.*, **24**, 196 (2015).
19. K. Baek and J.-W. Yang, *Chemosphere*, **57**, 1091 (2004).
20. M. Nadeem, M. Shabbir, M. A. Abdullah, S. S. Shah and G. McKay, *Chem. Eng. J.,* **148**, 365 (2009).
21. H. D. Choi, W. S. Jung, J. M. Cho, B. G. Ryu, J. S. Yang and K. Baek, *J. Hazard. Mater.*, **166**, 642 (2009).
22. S. Y. Lagergren, *Handlingar*, **24**, 1 (1898).
23. Y. S. Ho and G. McKay, *Process Biochem.*, **34**, 451 (1999).
24. K. Y. Foo and B. H. Hameed, *Chem. Eng. J.*, **156**, 2 (2010).
25. I. Langmuir, *J. Am. Chem. Soc.*, **40**, 1361 (1918).
26. F. H. Freundlich, *Z. Phys. Chem.*, **57**, 384 (1906).
27. R. R. Krug, W. G. Hunter and R. A. Grieger, *J. Phys. Chem.*, **80**, 2335 (1976).
28. G. Bai, M. Nichifor, A. Lopes and M. Bastos, *J. Phys. Chem. B*, **109**, 518 (2005).
29. W. Weber and J. Morris, *J. Sanit. Eng. Div.*, **89**, 31 (1963).
30. B. H. Ketelle and G. E. Boyd, *J. Am. Chem. Soc.*, **69**, 2836 (1947).
31. S. Han, F. Zhao, J. Sun, B. Wang, R. Wei and S. Yan, *J. Magn. Magn. Mater.*, **341**, 133 (2013).
32. J. Hu, D. Shao, C. Chen, G. Sheng, X. Ren and X. Wang, *J. Hazard. Mater.*, **185**, 463 (2011).
33. J. Fujiki and E. Furuya, *Fuel*, **164**, 180 (2016).